# Electric field-induced acoustic-optic mode coupling in an anticlinic liquid crystal

Shiyong Zhang,[1] S. S. Keast,[2] M. E. Neubert,[2] Rolfe G. Petschek,[1] and Charles Rosenblatt[1]
[1]*Department of Physics, Case Western Reserve University, Cleveland, Ohio 44106*
[2]*Liquid Crystal Institute, Kent State University, Kent, Ohio 44242*
(Received 14 June 2000)

A dc electric field was applied perpendicular to the tilt plane of a pitch-compensated (unwound helix) anticlinic liquid crystal. By means of quasielastic light scattering, the field was found to couple the acoustic and optic Goldstone modes, resulting in an increase of the relaxation time $\tau_\beta$ of the acousticlike eigenmode. Elastic constants were estimated from the relaxation time data.

PACS number(s): 61.30.Gd

Anticlinic liquid crystals (ALCs), which were first studied by Chandani *et al.* [1], exhibit a seemingly endless variety of scientifically interesting and technologically useful phenomena. In the chiral anticlinic phase, sometimes known as the smectic-$C_A^*$ phase, the molecular director tilts in the *x*-*y* plane by polar angle $\theta$ with respect to the smectic layer normal (the *y* axis); the associated azimuthal orientation in layer *j* is $\varphi_j$. For an unwound (infinite pitch) ALC the quantity $\Delta\varphi \equiv [\varphi_{j+1} - \varphi_j] = \pi$ (Fig. 1); for a chiral ALC having a finite pitch, however, $\Delta\varphi$ differs from $\pi$ typically by 1–2 %. Additionally, there exists a polarization $\vec{P}_j$ of magnitude *P* in layer *j* that lies perpendicular to the molecular tilt plane, where the azimuthal orientation of $\vec{P}$ also changes by $\Delta\varphi \approx \pi$ from one layer to the next (Fig. 1). For a finite helical pitch $\vec{P}_{j+1}$ and $\vec{P}_j$ are not quite antiparallel, and there exists a nonzero polarization when averaged over several layers. Thus, when subjected to a weak electric field, the helix continuously distorts [2]. For a pitch-compensated (unwound helix) ALC, where $\Delta\varphi = \pi$, $\vec{E}$ is parallel to $\vec{P}_{j+1}$ but antiparallel to $\vec{P}_j$. (Note too, that symmetry requires a polarization parallel to both the tilt plane and smectic layers, alternating in aziumthal direction by an angle $\pi$ from one layer interface to the next in an infinite-pitch ALC [3]. Such polarizations, which go under several monikers including $P_x$ [4] and $P_1$ [3,5], must always be antiparallel in adjacent layers in an infinite-pitch ALC, and thus will not contribute to our free energy below and will therefore be neglected.) For sufficiently large field, Zhang *et al.* reported that, instead of a continuous variation of $\varphi_j$ with field, a sharp Fréedericksz-like transition occurs at $E = E_{\rm th}$ [6], where the applied field overcomes both the elasticity and the anticlinic interactions. In this Rapid Communication we explore the behavior of director fluctuations below the Fréedericksz transition ($E < E_{\rm th}$), where the field tends to quench azimuthal fluctuations in layer $j+1$ but destabilize the azimuthal orientation of layer *j*, resulting in a coupling of the acoustic and optic Goldstone modes. Our central result is that the acousticlike mode decay time $\tau_\beta$ increases with electric field, a signature of a field-induced mixing of the optic and acoustic modes. Additionally, we are able to extract approximate elastic constants associated with the distortion.

Consider the geometry shown in Figs. 1 and 2. In previous work that considered the *joint* motion of tilted molecules in adjacent smectic layers, the free energy of the system was given by $F = (NL/2)\int_0^W \int_0^d f_{pair}\, dx\, dz$. Here *L* is the smectic layer thickness, *d* is the cell thickness, *W* is the width of the cell, *N* is the number of smectic layers, and $f_{pair}$ is the free energy density for a pair of adjacent layers given by

$$f_{pair} = PE\cos(\Delta\alpha + \Delta\beta) - PE\cos(\Delta\alpha - \Delta\beta) + 2U(1 - \cos 2\Delta\alpha).$$

$\Delta\beta$ corresponds to the azimuthal fluctuations of the symmetry axis for a pair of molecules in adjacent layers (Fig. 2), $\Delta\alpha$ corresponds to half the deviation from perfect anticlinic order, i.e., $\Delta\alpha = \frac{1}{2}(\pi - \Delta\varphi)$, and *U* is the anticlinic interaction coefficient. Note that the dielectric anisotropy contribution to $f_{pair}$, which is proportional to $\Delta\varepsilon E^2$, has been omitted because it is small.

In this paper we will consider both acoustic and optic modes that vary in space. In doing so we will introduce elastic constants that are independent of the type of mode, i.e., that are not dependent on whether the mode is acoustic or optic, but rather depend only on the *direction* of wave vector $\vec{q}$. It is not obvious that the elastic constants should be mode-independent, as some mechanisms and, more specifically, terms in the free energy of the form $\cos 2\Delta\alpha$ result in different elasticities for these two modes. However, other mechanisms including intralayer couplings, next-nearest-layer couplings, and terms in the free energy of the form

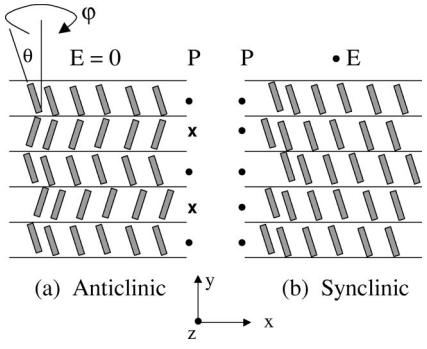


FIG. 1. (a) Schematic representation of anticlinic (smectic-$C_A^*$) phase for an infinitely long helical pitch at electric field $E = 0$. $\theta$ corresponds to the polar tilt angle of the molecules and *P* corresponds to the layer polarization. For sufficiently large electric field *E*, a transition to the synclinic (smectic-*C**) phase (b) occurs.

 

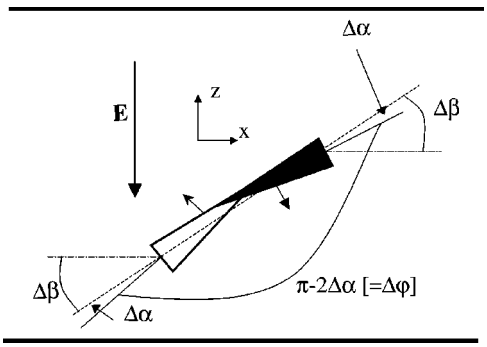


FIG. 2. Figure 1(a) rotated by 90°, showing an acoustic rotation $\beta$ and optic rotation $\alpha$.

$\cos 4\Delta\alpha$ result in identical contributions for these, in principle distinct, elasticities. Because very similar elasticities are consistent with the data presented below, we will assume that they do not depend on whether the distortion is opticlike or acousticlike. We therefore introduce two such elastic constants, $B_y$ and $B_z$, the elastic constants for long wavelength azimuthal fluctuations that vary respectively along the $y$ axis (corresponding to the layer normal) and those that vary along the $z$ axis, which are parallel to both the smectic layers and to the cell normal. If the system were viewed as a nematic, $B_y$ would correspond to a combination of bend and twist distortions, and $B_z$ to a splaylike distortion. Note that variations along the $x$ axis are not considered, as the light scattering geometry is chosen to exclude these wave vectors.

We will now suppose that the variables $\Delta\alpha$ and $\Delta\beta$ are slowly varying and continuous, and that we can approximate the sum over all pairs by an appropriate integral over all space. We will also assume that the associated elastic constants are the same for both the acoustic ($\Delta\beta$) and optic ($\Delta\alpha$) modes, resulting in a free energy

$$F=\int \tfrac{1}{2}\{f_{pair}+B_z[(\partial\Delta\beta/\partial z)^2+(\partial\Delta\alpha/\partial z)^2] + B_y[(\partial\Delta\beta/\partial y)^2+(\partial\Delta\alpha/\partial y)^2]\}dxdzdy.$$

We are interested in the dynamic behavior of the system. In order to calculate this behavior we shall assume that the only hydrodynamic modes that significantly affect the dynamics involve $\Delta\alpha$ and $\Delta\beta$, i.e., we can safely ignore the velocity or fluid motion and the layer undulations. With these assumptions we may write the two kinetic equations

$$d\Delta\alpha(\vec{r})/dt=\nu_{\alpha\alpha}\delta F/\delta\Delta\alpha(\vec{r})+\nu_{\alpha\beta}\delta F/\delta\Delta\beta(\vec{r}),$$

$$d\Delta\beta(\vec{r})/dt=\nu_{\beta\beta}\delta F/\delta\Delta\beta(\vec{r})+\nu_{\alpha\beta}\delta F/\delta\Delta\alpha(\vec{r}),$$

where $\nu_{ij}$ are kinetic coefficients. As $\Delta\alpha$ and $\Delta\beta$ correspond to the azimuthal angles of the anticlinic and synclinic order parameters, respectively, the kinetic coefficent $\nu_{\alpha\beta}$ must be zero, at least if the anticlinic order parameter is not too large. Additionally, we shall make the simplifying assumption that $\nu_{\alpha\alpha}=\nu_{\beta\beta}\equiv\eta^{-1}$, which implies that intralayer contributions dominate in the the kinetic coefficient. Finally we shall choose $\eta$ in such a way as to reproduce the conventional results for the smectic-$C$ phase for appropriate $\Delta\alpha$ and $\Delta\beta$. Expanding these equations for small $\Delta\alpha$ and $\Delta\beta$ and performing a spatial Fourier transform, we obtain

$$d\Delta\alpha_{\vec{q}}/dt=\eta^{-1}[-PE\Delta\beta_{\vec{q}}+(4U+B_yq_y^2+B_zq_z^2)\Delta\alpha_{\vec{q}}],$$

$$d\Delta\beta_{\vec{q}}/dt=\eta^{-1}[-PE\Delta\alpha_{\vec{q}}+(B_yq_y^2+B_zq_z^2)\Delta\beta_{\vec{q}}].$$

Upon diagonalizing these equations we find that there are two exponential relaxation rates given by

$$\tau^{-1}=\eta^{-1}[(2U+B_yq_y^2+B_zq_z^2)\pm 2(U^2+\tfrac{1}{4}P^2E^2)^{1/2}]. \quad (1)$$

For an experimental geometry that selects only the acoustic mode at $E=0$, application of an electric field results in a change of the eigenvectors with an attendant small contribution of opticlike fluctuations to the scattering signal. Thus, even though the slower $(-)$ acousticlike relaxation mode in Eq. (1) dominates the scattering signal, a small contribution to the scattering comes about at $E\neq 0$ from the fast $(+)$ opticlike mode. This opticlike contribution to the scattering is proportional to the square of the mixing of the modes, that is proportional to $P^2E^2/U^2$ for small $E$. It therefore results in a fractional change, proportional to $(U^2/P^2E^2)(\tau_\beta^{-1}/\tau_\alpha^{-1})$, of the relaxation rate measured for this geometry. Here $\tau_\alpha^{-1}$ and $\tau_\beta^{-1}$ are the relaxation rates for the fast and slow modes, respectively, given by Eq. (1). Thus, provided that $U/(B_yq_y^2+B_zq_z^2)$ is large, the change in the measured relaxation rate will be dominated by the field-dependent change in the relaxation rate of the acousticlike mode. Moreover, this dominance increases as the ratio of relaxation times [cf. Eq. (1)] increases. Thus, we are confident that our measured slow relaxation rate corresponds predominantly to acousticlike fluctuations, and we expand the slower relaxation rate in Eq. (1) for small $E$ and obtain

$$\tau_\beta^{-1}=\frac{B_yq_y^2+B_zq_z^2}{\eta}-\frac{P^2E^2}{4\eta U}. \quad (2)$$

The term involving the anticlinic coefficient $U$ indicates that this acousticlike mode, in which adjacent layers rotate *nearly* in tandem, involves a coupling between a pure acoustic and a pure optic mode. Additionally, we see that the relaxation rate $\tau_\beta^{-1}$ decreases, and thus the acousticlike mode becomes slower, with increasing field. (As an aside, we note that for $E>E_{\rm th}$ the equilibrium polarizations in adjacent layers are no longer antiparallel to each other, resulting in a quenching of the net polarization by the field and a concomitant increase in relaxation rate $\tau_\beta^{-1}$. This work will be presented elsewhere [7].)

We shall now discuss quasielastic light scattering measurements of the acousticlike relaxation rate $\tau_\beta^{-1}$. Cells were prepared by spin-coating two pairs of clean indium-tin-oxide (ITO) coated glass slides and baking. The coated slides were then rubbed with a cotton cloth using a dedicated rubbing machine and then placed together, separated by a pair of Mylar spacers with a nominal thickness of 12 $\mu$m. The cells were cemented and filled in the isotropic phase with a binary mixture of 4-(1-trifluoromethylhexyloxy-carbonyl)phenyl 4-octyloxybiphenyl 4-carboxylate [(R)-TFMHPOBC] [8] and 4-(1-methylheptyloxycarbonyl)phenyl 4′-octyloxybiphenyl-4-carboxylate [(R)-MHPOBC] [1]. The polariza-

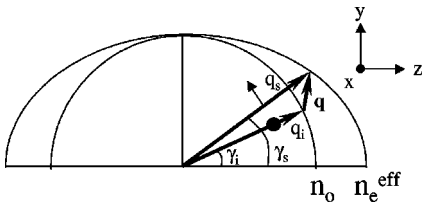


FIG. 3. Schematic representation of the scattering geometry (not to scale). Shown are the refractive index ellipsoid for the ordinary ($n_o$) and effective extraordinary ($n_e^{eff}$) indices, the incident wave vector $q_i$, scattered wave vector $q_s$, and their polarizations ● and →, respectively.

tions of these materials add constructively, but their helices wind in opposite directions [9]. Previously we had found that a 70:30 wt.% mixture of (R)-TFMHPOBC and (R)-MHPOBC provides an extremely long pitch that easily could be surface-stabilized in the bookshelf geometry [10]. Each cell was then slowly cooled through the isotropic–smectic-$A$ phase transition at 138 °C through the smectic-$A$–smectic-$C_A^*$ transition at 117 °C and stabilized at 111 °C in the anticlinic phase. The cooling rate was about 1 °C per hour to form a good planar alignment in the cell.

The cell was placed in our light scattering apparatus, described in detail in Ref. [11]. The sample was oriented so that the $y$-$z$ plane corresponded to the plane of scattering, as shown in Fig. 3, and was illuminated with light at wavelength 488 nm from an Argon-ion laser whose (ordinary) polarization was along the $x$ axis. Extraordinary polarized scattered light (this corresponds to a ''VH'' scattering geometry) was selected by an analyzer and detected by a photomultiplier tube, amplifier-discriminator, and Brookhaven Instruments BI-9000 digital autocorrelator. Since acousticlike fluctuations couple the $x$ component of polarization with the $y$ and $z$ components, and opticlike fluctuations do not involve the $x$ component of polarization, our geometry is sensitive only to acousticlike fluctuations. The scattering wave vector was determined from the incident and scattered angles $\gamma_i$ and $\gamma_s$ (external to the cell), the incident and scattered optical polarizations, and the refractive indices of the liquid crystal [10]. Owing to unavoidable fixed defects in the sample, the experiment was performed in the heterodyne mode.

A determination of the applied field $E$ was complicated by the very high resistance of polyimide (PI) layers which, despite the high resistance of the 12 $\mu$m liquid crystal layer ($>1$ MΩ), dominated the resistance of the cell [6]. Thus, for an applied dc voltage $V^{dc}$, most of the voltage drop occurred across the polyimide layer, and we could not use $V^{dc}/d$ as the field across the liquid crystal layer, where $d$ is the cell thickness. To overcome this difficulty, we examined both the dc Fréedericksz transition threshold voltage $V_{\rm th}^{dc}$ and the ac threshold $V_{\rm th}^{ac}$ [6], such that the ac measurement was performed at a frequency sufficiently high that charge buildup at the interfaces was deemed not to be a problem. Thus, for the ac case, the electric fields across the thin polyimide layers and the much thicker liquid crystal layer were determined by their dielectric constants (which are similar) and their thicknesses, and therefore the ac field across the liquid crystal could be taken as $E^{ac} \approx V^{ac}/d$ [6]. Thus, the dc field $E^{dc}$ across the liquid crystal was taken as $(V_{\rm th}^{ac}/V_{\rm th}^{dc})V^{dc}/d$.

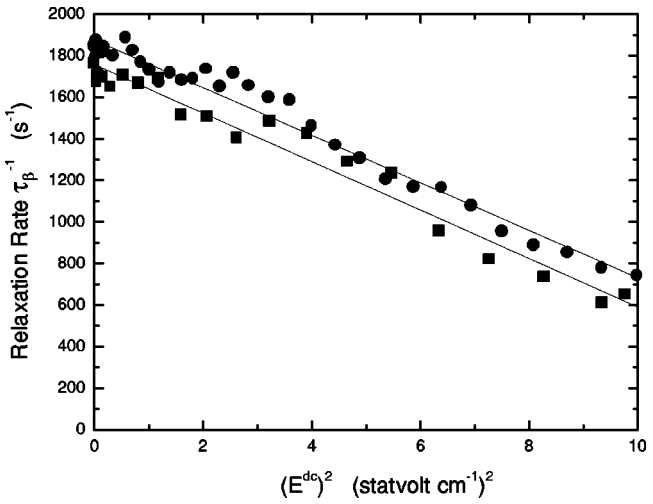


FIG. 4. Decay rate $\tau_\beta^{-1}$ vs the square of electric field $(E^{dc})^2$ for $\gamma_s = 37°$ (■) and $\gamma_s = 41°$ (●).

Figure 4 shows $\tau_\beta^{-1}$ versus $(E^{dc})^2$ for two different scattering angles. Note that the scatter in the data is due to a combination of the small signal-to-noise ratio and the brief ($\sim 1$ h) sampling periods for each value of field, which was necessary to prevent chemical degradation of the liquid crystal. For one set of measurements, $\gamma_i = 33°$ and $\gamma_s = 37°$, resulting in putative scattering wavevectors of $q_y = 7.2 \times 10^3$ cm$^{-1}$ and $q_z = 6.5 \times 10^3$ cm$^{-1}$; for the second set of data, $\gamma_i = 33°$ and $\gamma_s = 41°$, and thus $q_y = 1.4 \times 10^4$ cm$^{-1}$ and $q_z = 3.0 \times 10^3$ cm$^{-1}$. Both data sets exhibit the expected linear behavior in $(E^{dc})^2$ that occurs for $E < E_{\rm th}$, and the two fitted lines are not surprisingly parallel to each other, both having slopes $P^2/4\eta U$. The difference in the $y$ intercepts at $(E^{dc})^2 = 0$ is due to differences in the scattering wave vectors and elastic constants. The data clearly show a decrease in relaxation rate of the acousticlike mode with increasing electric field, indicative of coupling to optic fluctuations.

Approximate elastic constants may be extracted by considering the ratio $R$ of the $y$ intercept [$(1756 \pm 25)$ s$^{-1}$ and $(1874 \pm 15)$ s$^{-1}$ for data sets one and two, respectively] to the slope of $\tau_\beta^{-1}$ [$(115 \pm 4)$ statvolt$^2$ cm$^{-2}$ s$^{-1}$] in Eq. (2), viz., $R = 4U(B_y q_y^2 + B_z q_z^2)/P^2$. We have previously measured both $U$ and $P$ for this mixture at $T = 111$ °C, finding $P = 330$ esu cm$^{-2}$ (corresponding to 110 nC cm$^{-2}$) and $U = 2.1 \times 10^{-4}$ ergs cm$^{-3}$ at this temperature [10]. The actual scattering from this finite-sized system cannot, of course, be described solely in terms of these putative scattering wave vectors. Specifically $q_z d/\pi$ is approximately 1 and 2 for our scattering wave vectors. Thus, we believe that we are actually probing several wave numbers $q_z$ in our experiment, with the $z$ component of the scattering vector determined by the boundary conditions of the cell. Our results, therefore, should not be construed as giving precise values for the elastic constants; rather, they give reasonable first estimates. Thus, the two data sets together provide two equations in two unknowns, from which we obtain $B_y = (0.89 \pm 0.03) \times 10^{-7}$ dyn and $B_z = (3.6 \pm 0.2) \times 10^{-7}$ dyn. The error bars represent experimental data scatter, rather than the larger error due to the range of $q_z$ probed in the experiment. We note

that for the smectic-$C$ phase $B_y = K_{22} \sin^4\theta + K_{33} \sin^2\theta \cos^2\theta$ and $B_z = K_{11} \sin^2\theta$ [12], and $\theta = 24.5°$ at this temperature [10], where $K_{11}$, $K_{22}$, and $K_{33}$ correspond to the splay, twist, and bend nematic elastic constants, respectively. Thus, our measured value of $B_z$ would correspond to a splaylike elastic constant in the nematic phase of approximately $2\times10^{-6}$ dyn, a very reasonable value. On dividing our measured value of $B_y$ by $\sin^2\theta$, we obtain $K_{22}\sin^2\theta + K_{33}\cos^2\theta \sim 0.5\times10^{-7}$ dyn, a value comparable to a typical twist elastic constant, although a bit smaller than might be expected for a typical nematic bend elastic constant (which should be the dominant term in $B_y$ because $\cos^2\theta \sim 0.83$). Molecular shape-induced reductions of $K_{33}$ have been demonstrated for molecules having an inherently bent shape [13–15], although we do not believe that this is the operative mechanism here. The basis for the observed elastic constants as well as improved methods for measuring them will be the subject of future investigations.

To summarize, we studied the acousticlike director fluctuations for electric fields below the Fréedericksz transition threshold. The decay rate $\tau_\beta^{-1}$ for acousticlike fluctuations shows a linear dependence on $E^2$, consistent with a coupling of acoustic and optic Goldstone fluctuations. Approximate elastic constants were obtained from the measurements performed at two different scattering angles.

The authors are indebted to Bing Wen and X.-Y. Wang for useful conversations. This work was supported by the National Science Foundation under Grant No. DMR-9982020, and by the National Science Foundation's Advanced Liquid Crystalline Optical Materials Science and Technology Center under Grant No. DMR-8920147.

[1] A.D.L. Chandani, T. Hagiwara, Y. Suzuki, Y. Ouchi, H. Takezoe, and A. Fukuda, Jpn. J. Appl. Phys. **27**, L729 (1988).
[2] Y.P. Panarin, O. Kalinovskaya, and J.K. Vij, Liq. Cryst. **25**, 241 (1998).
[3] P.E. Cladis and H.R. Brand, Liq. Cryst. **14**, 1327 (1993).
[4] A. Fukuda, S.S. Seomun, T. Takahashi, Y. Takanishi, and K. Ishikawa, Mol. Cryst. Liq. Cryst. **303**, 379 (1997).
[5] X.Y. Wang, J.-F. Li, E. Gurarie, S. Fan, T. Kyu, M.E. Neubert, S.S. Keast, and C. Rosenblatt, Phys. Rev. Lett. **80**, 4478 (1998).
[6] S. Zhang, B. Wen, S.S. Keast, M.E. Neubert, P.L. Taylor, and C. Rosenblatt, Phys. Rev. Lett. **84**, 4140 (2000).
[7] B. Wen, S. Zhang, S.S. Keast, M.E. Neubert, P.L. Taylor, and C. Rosenblatt (unpublished).
[8] Y. Suzuki, T. Hagiwara, I. Kawamura, N. Okamura, T. Kitazume, M. Kakimoto, Y. Imai, Y. Ouchi, H. Takezoe, and A. Fukuda, Liq. Cryst. **6**, 167 (1989).
[9] J. Li, H. Takezoe, A. Fukuda, and J. Watanabe, Liq. Cryst. **18**, 239 (1995).
[10] M. Kimura, D.S. Kang, and C. Rosenblatt, Phys. Rev. E **60**, 1867 (1999).
[11] G.A. Dilisi, C. Rosenblatt, A.C. Griffin, and U. Hari, Phys. Rev. A **45**, 5738 (1992).
[12] P.G. DeGennes and J. Prost, *The Physics of Liquid Crystals* (Clarendon, Oxford, 1994).
[13] G.A. Dilisi, C. Rosenblatt, and A.C. Griffin, J. Phys. II **2**, 1065 (1992).
[14] G.A. Dilisi, E.M. Terentjev, A.C. Griffin, and C. Rosenblatt, J. Phys. II **3**, 597 (1993).
[15] M.R. Dodge, C. Rosenblatt, R.G. Petschek, M.E. Neubert, and M.E. Walsh, Phys. Rev. E (to be published).